
Adiabatic formulation of large-scale models of the atmosphere

Finite-difference schemes for the horizontal discretization. April 1994

By **A. J. Simmons**

European Centre for Medium-Range Forecast

Table of contents

- 1 . Introduction
- 2 . Distribution of grid-points
- 3 . Staggering of variables
 - 3.1 Staggered grids
 - 3.2 The linearized shallow-water equations on an f-plane
 - 3.2 (a) Discretizations of the linearized shallow-water equations
 - 3.3 The time-staggered D (Eliassen) grid
 - 3.4 Grid splitting
 - 3.5 Applications
- 4 . Conservation and Eulerian advection schemes
 - 4.1 Introduction
 - 4.2 The shallow-water equations on the sphere
 - 4.3 A conserving finite-difference scheme for the shallow-water equations on the sphere.
 - 4.4 Some other conserving schemes
- 5 . Treatment of the poles
 - 5.1 Formulation of the finite-difference scheme
 - 5.2 Computational stability

REFERENCES

1. INTRODUCTION

Three types of method are available for the horizontal discretization of the governing equations of large-scale models of the atmosphere. These are the finite-difference method, the spectral method and the finite-element method. The basics of these methods have been introduced in the preceding course on numerical methods.

All three methods are used today for operational numerical weather prediction. The spectral method is adopted al-

most universally for global medium-range forecasting models. Of the principal current operational models, the only one not using the spectral method is the finite-difference model of the United Kingdom Meteorological Office (Cullen and Davies, 1991). Some other centres are, however, considering future use of the finite-difference approach. More diversity is seen among the models employed for global climate modelling, but again the spectral method predominates; of 29 models listed by Gates(1992) as participating in AMIP, a model comparison project, 19 were spectral. Conversely, for local, short-range forecasting, limited-area finite-difference models are most commonly used. However, a spectral limited-area model has been used operationally by the Japan Meteorological Agency for a number of years (Tatsumi, 1986), and Météo-France has recently implemented a global spectral model with non-uniform resolution for this purpose (Courtier and Geleyn, 1988). Spectral limited-area models have also been developed by several other groups: HIRLAM, ECMWF, Météo-France and NMC, Washington (Haugen and Machenhauer, 1993; Hoyer, 1987; Juang and Kanamitsu, 1994). The finite-element method has been in operational use for regional prediction for some time in Canada, and a multi-purpose model based on the method with option of variable resolution is under development for uses which include global prediction (Côté et al., 1993).

A number of choices have to be made once it has been decided to use the finite-difference method for an atmospheric model. Particular choices may depend on other decisions made for the model, particularly the choice of time-stepping method, for example whether a semi-implicit or split-explicit scheme is chosen to handle fast-moving gravity-waves, or whether an Eulerian or semi-Lagrangian scheme is chosen for advection. Questions to be answered include:

- How should grid points be distributed over the sphere?
- How should variables be staggered?
- Which finite-difference scheme should be used?
 - Which conservation properties should be satisfied?
 - Which order of accuracy should be used?
- How should the special problems of the poles be treated?

In this lecture, we discuss how some of these questions have been answered for different models.

2. DISTRIBUTION OF GRID-POINTS

The problem of how to distribute grid points over the sphere has yet to be solved in a fully satisfactory manner. The generally accepted method for medium-range prediction and longer term integrations is to use a grid which is regular in latitude and longitude, as in the upper illustration of Fig. 1 . Such a grid was used in the original operational ECMWF model (Burridge, 1980; Simmons et al., 1989), and is used today in the UKMO model. In this case the grid length becomes small in the zonal direction close to the poles, and special calculations may have to be carried out to avoid having to use a very small time-step, as discussed in Subsection 5. Unnecessary expense may also be incurred in calculating physical parametrizations on a grid which is overly fine in the east-west close to the poles.

These inefficiencies were recognized in the early days of global modelling, and led Kurihara(1965) to propose use of the “skipped” or “Kurihara” grid shown in the middle illustration of Fig. 1 . However, problems were encountered in practice with these grids, most notably in the tendency for spuriously high pressure to develop at the poles. Their use has been largely abandoned in finite-difference models, although more recently Purser(1988) has suggested their reintroduction, but using more accurate numerical schemes to remedy the problems. The use of an icosahedral grid (see also Fig. 1) has also been considered (e.g. Williamson, 1970; see also Cullen, 1974, for the finite-element method), but has not gained widespread acceptance.

The traditional method of avoiding problems at or near the pole in limited-area models was to use projection onto a plane, typically a polar stereographic projection. More recent models tend to use a regular latitude/longitude sys-

tem, but with the pole of the coordinate system rotated away from the geographic pole so that the equator of the rotated system passes through the domain of interest. This is the approach now in use at the UKMO, in the HIRLAM and DWD models, and in the “eta” model of NMC, Washington (see papers in Proceedings of 1991 ECMWF Seminar, and Mesinger et al., 1988).

Reference was made in the introduction to variable resolution spectral and finite-element models designed primarily for local short-range prediction. An example of such (fixed) variable resolution in a finite-difference model is described by Sharma et al. (1987). Another possibility is adaptive mesh refinement in which resolution is refined where the solution has fine-scale structure, rather than in a fixed region. Among the review articles listed in the Reference section is one by Skamarock on this topic.

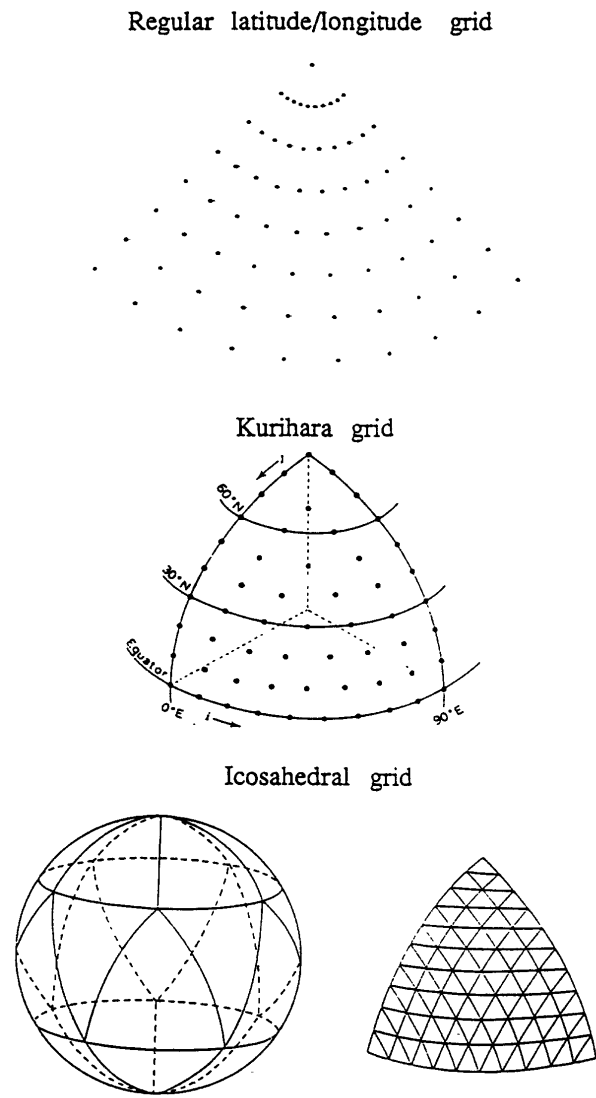


Figure 1. Alternative distributions of grid points on the sphere

3. STAGGERING OF VARIABLES

3.1 Staggered grids

Having decided on the basic distribution of grid points, a choice has to be made as to how to arrange the different prognostic variables on the grid, since the most obvious choice of representing all variables at the same point has disadvantages. In the following, the standard layouts are illustrated for the variables of the shallow-water equations, the zonal and meridional wind components, u and v , and the geopotential ϕ . In multi-level models, temperature and surface pressure are defined at the ϕ points. Humidity, any extra advected atmospheric variables, and surface variables are also generally held at the ϕ points in comprehensive atmospheric models, as is salinity in ocean models.

There are five principal arrangements of variables, usually identified by the letters A to E (see, for example, [Arakawa](#) and Lamb, 1977). The A grid is the basic unstaggered grid illustrated in [Fig. 2](#), in which all variables are held at the same point. The B and E grids ([Figs. 3](#) and [6](#)) carry both wind components at the same points, and are referred to as semi-staggered. The C and D grids ([Figs. 4](#) and [5](#)) provide two fully staggered layouts in which there are different locations for the two wind components and for height. Note that the E grid can be viewed as the B grid rotated through 45° .

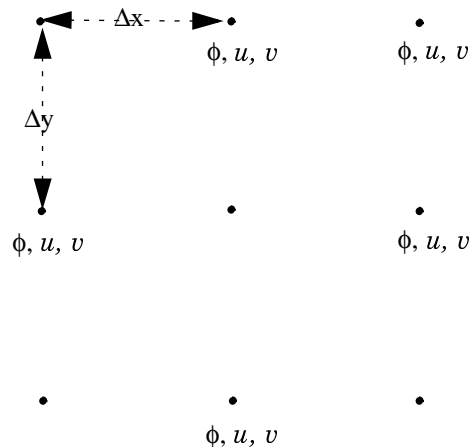


Figure 2. Distribution of variables for the unstaggered A grid

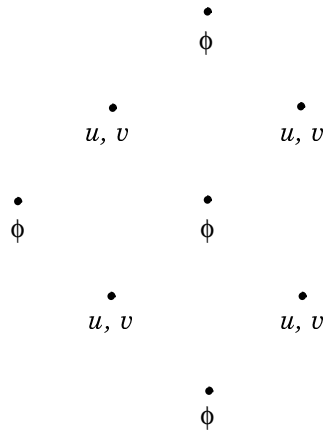


Figure 3. Distribution of variables for the staggered B grid

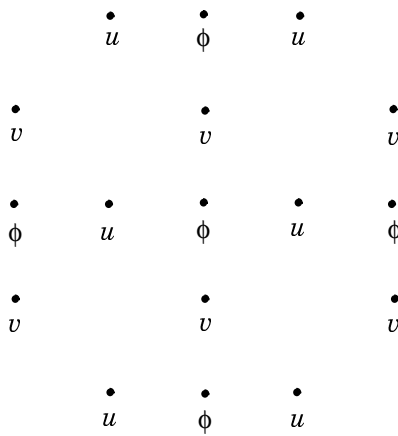


Figure 4. Distribution of variables for the staggered C grid

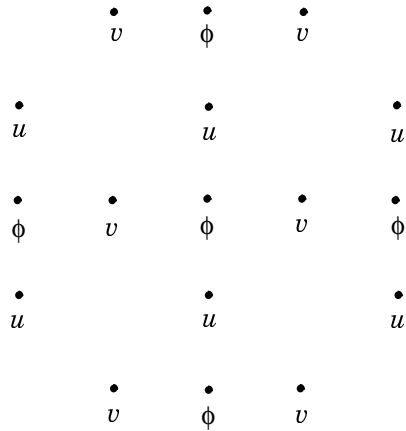


Figure 5. Distribution of variables for the staggered D grid

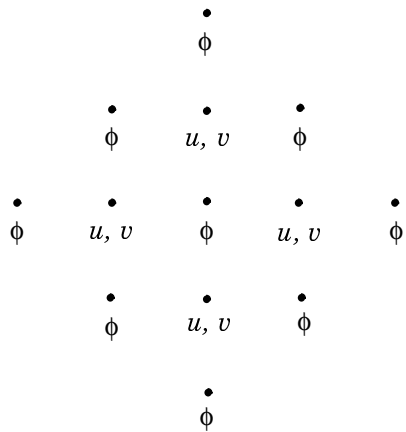


Figure 6. Distribution of variables for the staggered E grid

3.2 The linearized shallow-water equations on an f-plane

To illustrate the application of the various grids it is convenient to consider the linearized shallow-water equations on an f-plane:

$$\begin{aligned}\frac{\partial u}{\partial t} &= -\frac{\partial \phi}{\partial x} + fv \\ \frac{\partial v}{\partial t} &= -\frac{\partial \phi}{\partial y} - fu \\ \frac{\partial \phi}{\partial t} &= -\Phi \left(\frac{\partial u}{\partial x} + \frac{\partial v}{\partial y} \right)\end{aligned}$$

The choice of staggering may be closely linked with the choice of time scheme. One example is provided by the forward/backward (two-level) time scheme, as used for instance in the UKMO model:



$$\begin{aligned}\delta_t u &= -\frac{\partial}{\partial x}\phi(t-\Delta t) + f\bar{v}^t \\ \delta_t v &= -\frac{\partial}{\partial y}\phi(t-\Delta t) - f\bar{u}^t \\ \delta_t \phi &= -\Phi\left[\frac{\partial}{\partial x}u(t) + \frac{\partial}{\partial y}v(t)\right]\end{aligned}$$

Here $\delta_t u = \frac{1}{\Delta t}[u(t) - u(t - \Delta t)]$ and $\bar{u}^t = \frac{1}{2}[u(t) + u(t - \Delta t)]$

These equations are solved first for $u(t)$ and $v(t)$, and then for $\phi(t)$. The solution of the coupled implicit equations for the wind components is evidently simpler for the semi-staggered grids in which the two wind components are held at the same points.

For the semi-implicit (three-level) time scheme used, for example, in the original ECMWF finite-difference model, we have:

$$\begin{aligned}\partial_{2t} u &= -\frac{\partial}{\partial x}\bar{\phi}^{-2t} + fv(t) \\ \partial_{2t} v &= -\frac{\partial}{\partial y}\bar{\phi}^{-2t} - fu(t) \\ \partial_{2t} \phi &= -\Phi\left[\frac{\partial}{\partial x}\bar{u}^{2t} + \frac{\partial}{\partial y}\bar{v}^{2t}\right]\end{aligned}$$

Here $\partial_{2t} u = \frac{1}{2\Delta t}[u(t + \Delta t) - u(t - \Delta t)]$ and $\bar{u}^{2t} = \frac{1}{2}[u(t + \Delta t) + u(t - \Delta t)]$

This leads to a Helmholtz equation of the form:

$$\phi(t + \Delta t) - (2\Delta t)^2 \Phi \nabla^2 \phi(t + \Delta t) = \text{terms involving time levels } t \text{ and } t - \Delta t$$

to be solved for $\phi(t + \Delta t)$, after which $u(t + \Delta t)$ and $v(t + \Delta t)$ can be computed. The discretization of this Helmholtz equation is of simplest form when the C grid is used.

3.2 (a) Discretizations of the linearized shallow-water equations. We use the following notation for the second-order finite-difference derivative and averaging operators with respect to x :

$$\delta_x \phi = \frac{1}{\Delta x} \left[\phi\left(x + \frac{1}{2}\Delta x\right) - \phi\left(x - \frac{1}{2}\Delta x\right) \right]$$

and

$$\bar{\phi}^x = \frac{1}{2} \left[\phi\left(x + \frac{1}{2}\Delta x\right) + \phi\left(x - \frac{1}{2}\Delta x\right) \right]$$

with similar expressions for the independent variable y .

With these definitions, the simplest second-order discretizations of the linearized shallow water equations for the various staggered grids are given by:



A grid:

$$\begin{aligned}\frac{\partial u}{\partial t} &= -\delta_x \bar{\phi}^x + fv \\ \frac{\partial v}{\partial t} &= -\delta_y \bar{\phi}^y - fu \\ \frac{\partial \phi}{\partial t} &= -\Phi(\delta_x \bar{u}^x + \delta_y \bar{v}^y)\end{aligned}$$

B grid:

$$\begin{aligned}\frac{\partial u}{\partial t} &= -\delta_x \bar{\phi}^y + fv \\ \frac{\partial v}{\partial t} &= -\delta_y \bar{\phi}^x - fu \\ \frac{\partial \phi}{\partial t} &= -\Phi(\delta_x \bar{u}^y + \delta_y \bar{v}^x)\end{aligned}$$

C grid:

$$\begin{aligned}\frac{\partial u}{\partial t} &= -\delta_x \phi + f \bar{v}^{xy} \\ \frac{\partial v}{\partial t} &= -\delta_y \phi - f \bar{u}^{xy} \\ \frac{\partial \phi}{\partial t} &= -\Phi(\delta_x u + \delta_y v)\end{aligned}$$

D grid:

$$\begin{aligned}\frac{\partial u}{\partial t} &= -\delta_x \bar{\phi}^{xy} + f \bar{v}^{xy} \\ \frac{\partial v}{\partial t} &= -\delta_y \bar{\phi}^{xy} - f \bar{u}^{xy} \\ \frac{\partial \phi}{\partial t} &= -\Phi(\delta_x \bar{u}^{xy} + \delta_y \bar{v}^{xy})\end{aligned}$$

E grid:

$$\begin{aligned}\frac{\partial u}{\partial t} &= -\delta_x \phi + fv \\ \frac{\partial v}{\partial t} &= -\delta_y \phi - fu \\ \frac{\partial \phi}{\partial t} &= -\Phi(\delta_x u + \delta_y v)\end{aligned}$$

Several comments can be made on the above forms:



- (i) Since $\delta_x \bar{\phi}^x = \frac{1}{2\Delta x} [\phi(x + \Delta x) - \phi(x - \Delta x)]$ all derivatives in the A grid formulation are effectively taken over double grid lengths, with implied loss of accuracy.
- (ii) The form of the Coriolis terms for the B grid favours implementation of the forward/backward scheme illustrated in 3.2.
- (iii) Suitability of the C grid for implementation of semi-implicit time differencing has already been noted. Coriolis terms are averaged in both horizontal directions, thereby reducing the amplitude of these terms for small-scale motion.
- (iv) The extensive averaging in the discretization shown for the D grid can be avoided by time-staggering, as discussed below.
- (v) The E grid also favours implementation of the forward/backward scheme. In this case there is no averaging of right-hand side terms. However, comparing square grids of equal resolution, i.e. when the distance between neighbouring grid points carrying the same variable is the same for each grid, the x and y derivatives for the E grid are taken over a grid interval which is $\sqrt{2}$ longer than for the other staggered grids.

3.3 The time-staggered D (Eliassen) grid

Staggering variables in time as well as space provides a way of avoiding the averaging on the right-hand side terms indicated above for the D grid. This technique, due to Eliassen(1956), involves representing variables at every second time step on an offset D grid, illustrated in Fig. 7 . The shallow water equations are in this case discretized as shown above for the E grid. If the right-hand side terms are evaluated using variables on the D grid shown in Fig. 5 , then tendencies are computed for the variables at the positions shown on the offset grid (Fig. 7). On the next time step they are computed back on the original grid. A variant of this approach is to use a higher-order interpolation to transfer values back from the offset grid to the original grid (Bratseth, 1983).

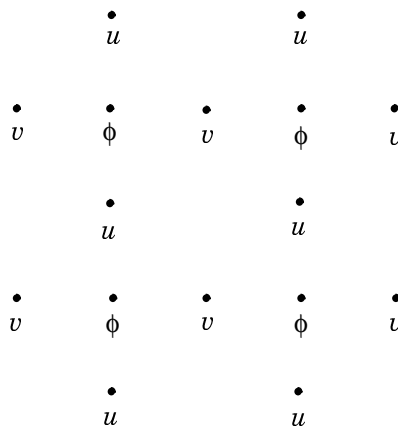


Figure 7. Distribution of variables for the offset time-staggered D (Eliassen) grid

3.4 Grid splitting

The B and E grids can be regarded as being made up of two C grids. This is illustrated below in Fig. 8 for the B grid. If no distinction is made between variables represented by upper- and lower-case characters, then the figure represents a B grid. However, half the points, those denoted by lower-case characters, form a C grid whose x and

y axes are rotated 45° anticlockwise relative to the axes of the B grid. The other half, denoted by upper-case characters, form a second C grid, shifted by one grid-length along the x - axis of the B grid.

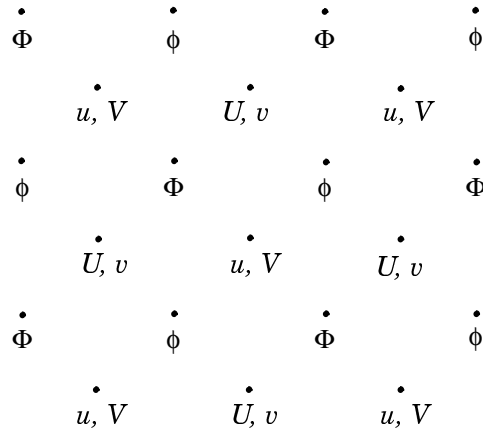


Figure 8. Distribution of variables on the B grid illustrating how it can be viewed as a combination of two C grids rotated through 45° , identified by variables written in upper and lower cases.

In formulating B- and E-grid models, action has to be taken to avoid solutions splitting into two separate distributions on the two C subgrids. One effective remedy, proposed by Mesinger(1973), is to modify the continuity equation by a formally small term:

$$\frac{\partial \phi}{\partial t} + \Phi(\delta_x \bar{u}^y + \delta \bar{v}^x) + w \Delta t \Phi(\nabla_+^2 - \nabla_x^2)\phi = 0$$

where ∇_+^2 and ∇_x^2 are two finite-difference forms of the Laplacian and w is an adjustable parameter. For a square grid ($\Delta x = \Delta y$) the two forms of the Laplacian are:

$$\nabla_+^2 = [-4\phi(x, y) + \phi(x + \Delta x, y) + \phi(x - \Delta x, y) + \phi(x, y + \Delta y) + \phi(x, y - \Delta y)] / (\Delta x)^2$$

and

$$\nabla_x^2 = \frac{1}{2}[-4\phi(x, y) + \phi(x + \Delta x, y + \Delta y) + \phi(x - \Delta x, y + \Delta y) + \phi(x + \Delta x, y - \Delta y) + \phi(x - \Delta x, y - \Delta y)] / (\Delta x)^2$$

3.5 Applications

A number of idealized calculations have been carried out to assess the suitability of the various grids. Discussions of these can be found in several of the review articles cited in the list of references. A general result of these calculations is that the staggered grids are indeed to be preferred to the unstaggered A grid. Beyond this, no one staggered arrangement of variables appears to be overwhelmingly superior.

The lack of a clear winner from among the various staggered grids in idealized tests is reflected in the variety of grids used in operational finite-difference models. The B grid is currently used in the UKMO “unified” model, for climate simulation as well as numerical weather prediction. The C grid was chosen for the first operational ECMWF model, and is in operational use in the several countries that run versions of the HIRLAM model, whose



adiabatic formulation was derived from that of the original ECMWF model. This grid is also used in the operational limited-area models of DWD, and a C-grid version of the UKMO model is under development. The D grid is used in the DNMI model using interpolation from the offset D grid as discussed above. It is also used (with time-staggering) in NMC's "nested grid" model (Phillips, 1979). However, the E grid, for which schemes were developed extensively by Mesinger and Janji in Belgrade, is used in NMC's newer "eta" model. For reasons indicated above, the gravity-wave terms are generally handled by the semi-implicit method in the C-grid models, and by forward/backward time differencing in the B- and E-grid models. Overall, the C grid appears to be emerging as the most popular, with the E grid its closest competitor.

4. CONSERVATION AND EULERIAN ADVECTION SCHEMES

4.1 Introduction

There are several reasons why numerical schemes for models are often formulated to respect conservation properties of the governing equations. An important practical consideration is that satisfaction of conservation properties helps to ensure the computational stability of a model. Apart from this, the direct physical realism of a conservation property may be a desirable feature. For example, ensuring conservation of mass prevents the surface pressure from drifting to highly unrealistic values in long-term integrations of atmospheric models. Advection schemes which satisfy an appropriate dynamical conservation property may help to ensure the realism of a model's energy spectrum.

There are, however, considerations other than conservation that might influence the choice of numerical scheme. Shape-preservation (avoidance of the generation of spurious maxima or minima) may be considered an important feature of an advection scheme, and the economy of a method (especially the ability to take long time steps) may be a critical factor. Indeed, semi-Lagrangian advection schemes, generally without formal conservation properties, are increasingly being developed for numerical weather prediction.

4.2 The shallow-water equations on the sphere

To illustrate conservation and a conserving difference scheme it is convenient to consider the full shallow-water equations on the sphere. These can be written in the form:

$$\begin{aligned}\frac{\partial u}{\partial t} &= \frac{1}{\cos\theta} \left[-\frac{1}{a} \frac{\partial}{\partial \lambda} (\phi + E) + Z\phi v \cos\theta \right] \\ \frac{\partial v}{\partial t} &= -\frac{1}{a} \left[\frac{\partial}{\partial \theta} (\phi + E) - Z\phi u \right] \\ \frac{\partial \phi}{\partial t} &= -\frac{1}{a \cos\theta} \left[\frac{\partial}{\partial \lambda} (\phi u) + \frac{\partial}{\partial \theta} (\phi v \cos\theta) \right]\end{aligned}$$

where λ is longitude, θ is latitude and a is the radius of the sphere, with

$$E = \frac{1}{2}[u^2 + v^2]$$

and

$$Z = \frac{1}{\phi} \left[f + \frac{1}{a \cos \theta} \left\{ \frac{\partial v}{\partial \lambda} - \frac{\partial}{\partial \theta} (u \cos \theta) \right\} \right]$$

Here $f = 2\Omega \sin \theta$, with Ω the planetary rotation rate.

It can be verified that these equations are such that the following conservation relations hold:

Mass

$$\frac{\partial}{\partial t} \int_{-\pi/2}^{\pi/2} \int_0^{2\pi} \phi \cos \theta \, d\lambda d\theta = 0$$

Energy

$$\frac{\partial}{\partial t} \int_{-\pi/2}^{\pi/2} \int_0^{2\pi} \left(E\phi + \frac{\phi^2}{2} \right) \cos \theta \, d\lambda d\theta = 0$$

Potential enstrophy

$$\frac{\partial}{\partial t} \int_{-\pi/2}^{\pi/2} \int_0^{2\pi} Z^2 \phi \cos \theta \, d\lambda d\theta = 0$$

4.3 A conserving finite-difference scheme for the shallow-water equations on the sphere,

As an example of a conserving finite-difference scheme we take the C-grid scheme used in ECMWF's original operational model. This scheme conserves mass and potential enstrophy, following Sadourny (1975). The spatial discretization is given by:

$$\begin{aligned} \frac{\partial u}{\partial t} &= \frac{1}{\cos \theta} \left[-\frac{1}{a} \delta_\lambda (\phi + [E]) + [\overline{Z}]^\theta \overline{V \cos \theta}^{\theta\lambda} \right] \\ \frac{\partial v}{\partial t} &= -\frac{1}{a} \delta_\theta (\phi + [E]) - [\overline{Z}]^\lambda \overline{U}^{\theta\lambda} \\ \frac{\partial \phi}{\partial t} &= -\frac{1}{a \cos \theta} [\delta_\lambda (U) + \delta_\theta (V \cos \theta)] \end{aligned}$$

where the zonal and meridional mass fluxes, U and V , are given by

$$U = \overline{\phi}^\lambda u \quad \text{and} \quad V = \overline{\phi}^\theta v$$

with

$$[E] = \frac{1}{2} \left[\overline{u^{2\lambda}} + \frac{1}{\cos \theta} \overline{v^2 \cos \theta}^\theta \right]$$

and

$$[Z] = \frac{1}{\phi \cos \theta} \left[f \overline{\cos \theta}^\theta + \frac{1}{a} \{ \delta_\lambda v - \delta_\theta (u \cos \theta) \} \right]$$

Sadourny(1975) discusses how enstrophy conservation helps maintain a realistic energy spectrum. However, adding formal conservation properties does not *guarantee* stability. The scheme initially tested at ECMWF conserved energy also, but was unstable when applied in a multi-level model (Hollingsworth et al. 1983). The instability manifested itself in a catastrophic weakening of the simulated flow over a two to three day period, and was linked to a poorer momentum conservation in the energy-conserving version.

4.4 Some other conserving schemes

There is a quite extensive literature on conserving finite-difference schemes. The pioneering contributions of Arakawa began with a paper in 1966; a recent work (Arakawa and Hsu, 1990) presented C-grid schemes which conserve energy, but dissipate potential enstrophy. Janji (1984) derived an E-grid scheme with “built-in control” of energy cascade. This is a transform to the E-grid of a C-grid scheme of Arakawa which conserves energy and enstrophy for non-divergent flow. It is used today in the NMC “eta” model. A conserving B-grid scheme, following Mesinger (1981), with option of fourth-order accuracy, is used in the UKMO “unified” model (Cullen and Davies, 1991).

5. TREATMENT OF THE POLES

5.1 Formulation of the finite-difference scheme

Care is needed in the formulation of finite-difference schemes for the polar caps in global models. As an example, we take the ECMWF shallow-water scheme. The C grid is defined such that ϕ is held at the two polar points. Tendencies of ϕ are thus needed at these points, and polar values of $[E]$ and U also have to be defined, as they are needed to integrate the equation

$$\frac{\partial v}{\partial t} = -\frac{1}{a} \delta_\theta (\phi + [E]) - [Z]^\lambda \bar{U}^{\theta\lambda}$$

for values of v one half grid-length from the poles.

For the polar tendency of ϕ , the continuity equation

$$\frac{\partial \phi}{\partial t} = -\frac{1}{a \cos \theta} [\delta_\lambda (U) + \delta_\theta (V \cos \theta)]$$

is integrated over the polar cap, and Green's theorem is applied to give

$$\frac{\partial}{\partial t} \phi_{\text{pole}} = \frac{4S}{nlon a \Delta \theta} \sum_{i=1}^{nlon} V_{\text{pole} - \frac{1}{2}, i}$$

where the sum is of the meridional mass fluxes over all longitudes ($i = 1, 2, \dots, nlon$) one half grid-length from the pole, and $S = 1$ for the North Pole and $S = -1$ for the South Pole.

The polar values of $[E]$ and U are determined from considerations of conservation. The specific expressions are given by [Burridge](#) (1980), who also illustrates how the scheme performs well in representing Rossby–Haurwitz wave motion in the vicinity of a pole.

5.2 Computational stability

Another important requirement is to avoid a highly restrictive CFL time-step limit arising from the short east-west grid-lengths near the poles when a regular latitude/longitude grid is used.

The usual solution is based on Fourier decomposition poleward of critical latitudes. The unstable higher-wave-number components of tendencies or fields are modified, and the tendencies or fields are transformed back to grid-point values. Fourier filtering involves reducing the amplitudes of higher-wavenumber components of tendencies or fields by sufficient amounts to ensure stability. For example, the results presented by [Burridge](#) (1980) were obtained by filtering the tendency of wavenumber k by a factor:

$$\min\left[1, \frac{\cos\theta}{\cos(\pi/4)\sin(k\Delta\lambda/2)}\right]$$

Variants are:

- (i) Applying the filtering only to the most critical of the terms that make up the tendencies.
- (ii) Fourier chopping: a special case in which higher-wavenumber components of tendencies or fields are set to zero.
- (iii) Use of a scale-selective diffusion scheme with sufficient damping to prevent instability, as used in the former operational ECMWF model; if $X_p(t + \Delta t)$ is the provisional, undiffused new value of a variable, the implicit scheme is

$$\frac{1}{2\Delta t}[x(t + \Delta t) - X_p(t + \Delta t)] = -K\left[\frac{1}{a^4\cos^4\theta}\delta_\lambda^4 X(t + \Delta t) + \frac{1}{a^4}\delta_\theta^4 X_p(t + \Delta t)\right]$$

which is solved in Fourier space for the diffused value $X(t + \Delta t)$

The alternative of using a skipped or Kurihara grid was discussed in [Section 2](#). Another early approach was that of [Grimmer](#) and Shaw (1967), who used time-steps that were shorter near the poles than elsewhere. Recently, [Bates](#) et al. (1993) have shown that use of semi-Lagrangian advection obviates the need for Fourier filtering in a global model with regular latitude/longitude grid. However, it remains to be seen whether finite-difference models can be developed which approach the efficiency of spectral models which use the “reduced” grid of [Hortal](#) and Simmons (1991) (see also [Courtier](#), 1994), in which the longitudinal grid spacing is close to uniform over the sphere.

REFERENCES

1.1 Textbook:

[Haltiner](#), G.J. and R.T. Williams, 1979: Numerical Prediction and Dynamic Meteorology, 2nd ed., *Wiley*, 477pp.

5.3 Reviews:

GARP Publication Series No. 17, [WMO](#). (Vol. I, Mesinger and Arakawa, 1976; Vol.II, several authors, 1979)



Proceedings of 1983 ECMWF Seminar on Numerical Methods for Weather Prediction (especially papers by Janji_ & Mesinger, Arakawa, and Dell'Osso)

Proceedings of 1991 ECMWF Seminar on Numerical Methods in Atmospheric Models (especially papers by Cullen, Skamarock, Gustafsson, Majewski)

5.4 Specific papers referred to in the text:

Arakawa, A., 1966: Computational design for long-term numerical integrations of the equations of atmospheric motion. *J. Comput. Phys.*, 1, 119-143.

Arakawa, A. and V.R. Lamb, 1977: Computational design of the basic dynamical processes of the UCLA general circulation model. *Methods in computational physics*, 17, 173-265.

Arakawa, A. and Y.-J. Hsu, 1990: Energy conserving and potential-ensrophy dissipating schemes for the shallow-water equations. *Mon. Wea. Rev.*, 118, 1960-1969.

Bates, J.R., S. Moorthi and R.W. Higgins, 1993: A global multi-level atmospheric model using a vector semi-Lagrangian finite-difference scheme. *Mon. Wea. Rev.*, 121, 244-263.

Bratseth, A., 1983: Some economical explicit finite-difference schemes for the primitive equations. *Mon. Wea. Rev.*, 111, 663-668.

Burridge, D.M., 1980: Some aspects of large scale numerical modelling of the atmosphere. *Proceedings of 1979 ECMWF Seminar on Dynamical Meteorology and Numerical Weather Prediction*, Vol. 2, 1-78.

Côté, J., M. Roch, A. Staniforth and L. Fillion, 1993: A variable-resolution semi-Lagrangian finite-element global model of the shallow-water equations. *Mon. Wea. Rev.*, 121, 231-243.

Courtier, P., and J.-F. Geleyn, 1988: A global numerical weather prediction model with variable resolution: Application to shallow-water equations. *Quart. J. Roy. Meteor. Soc.*, 114, 1321-1346.

Courtier, P., 1994: A pole problem in the reduced Gaussian grid. *Quart. J. Roy. Meteor. Soc.*, 120, to appear in July issue.

Cullen, M.J.P., 1974: Integrations of the primitive equations on a sphere using the finite element method. *Quart. J. Roy. Meteor. Soc.*, 100, 555-562.

Cullen, M.J.P. and T. Davies, 1991: A conservative split-explicit integration scheme with fourth-order horizontal advection. *Quart. J. Roy. Meteor. Soc.*, 117, 993-1002.

Eliassen, A., 1956: A procedure for numerical integration of the primitive equations of the two-parameter model of the atmosphere. *Science Report 4, Department of Meteorology, UCLA*, 53pp.

Gates, W.L., 1992: AMIP: The Atmospheric Model Intercomparison Project. *Bull. Amer. Meteor. Soc.*, 73, 1962-1970.

Grimmer, M. and Shaw, D.B., 1967: Energy preserving integrations of the primitive equations on the sphere. *Quart. J. Roy. Meteor. Soc.*, 93, 337-349.

Haugen, J.E., and B. Machenhauer, 1993: A spectral limited-area model formulation with time-dependent boundary conditions applied to the shallow-water equations. *Mon. Wea. Rev.*, 121, 1786-1815.

Hollingsworth, A., P. Kållberg, V. Renner and D.M. Burridge, 1983: An internal symmetric computational instability. *Quart. J. Roy. Meteor. Soc.*, 109, 417-428.

Hortal, M., and A.J. Simmons, 1991: Use of reduced Gaussian grids in spectral models. *Mon. Wea. Rev.*, 119,



1057-1074.

Hoyer, J.-M., 1987: The ECMWF spectral limited area model. *Proceedings of ECMWF Workshop on Techniques for Horizontal Discretization in Numerical Weather Prediction Models*, 343-359.

Janji, Z.I., 1984: Nonlinear advection schemes and energy cascade on semi-staggered grids. *Mon. Wea. Rev.*, 112, 1234-1245.

Juang, H.-M. H., and M. Kanamitsu, 1994: The NMC nested regional spectral model. *Mon. Wea. Rev.*, 122, 3-26.

Kurihara, Y., 1965: Numerical integration of the primitive equations on a spherical grid. *Mon. Wea. Rev.*, 93, 399-415.

Mesinger, F., 1973: A method for construction of second-order accuracy difference schemes permitting no false two-grid-interval wave in the height field. *Tellus*, 25, 444-458.

Mesinger, F., 1981: Horizontal advection schemes on a staggered grid, an enstrophy and energy conserving model. *Mon. Wea. Rev.*, 109, 467-478.

Mesinger, F., Z.I. Janji, S. Nickovic, D. Gavrilov and D.G. Deaven, 1988: The step-mountain coordinate: Model description and performance for cases of Alpine lee cyclogenesis and for a case of an Appalachian redevelopment. *Mon. Wea. Rev.*, 116, 1493-1518.

Phillips, N.A., 1979: The nested grid model. *NOAA Technical Report NWS 22, Dept. of Commerce, Silver Spring, MD*, 80pp.

Purser, R.J., 1988: Accurate numerical differencing near a polar singularity of a skipped grid. *Mon. Wea. Rev.*, 116, 1067-1076.

Sadourny, R., 1975: The dynamics of finite-difference models of the shallow-water equations. *J. Atmos. Sci.*, 32, 680-689.

Sharma, O.P., H.C. Upadhyaya, T. Braine-Bonnaire and R. Sadourny, 1987: Experiments on regional forecasting using a stretched-coordinate general circulation model. *J. Meteor. Soc. Japan, Special Volume, Short and Medium Range Numerical Weather Prediction*, 263-271.

Simmons, A.J., D.M. Burridge, M. Jarraud, C. Girard and W. Wergen, 1989: The ECMWF medium-range prediction models: Development of the numerical formulations and the impact of increased resolution. *Meteor. Atmos. Phys.*, 40, 28-60.

Tatsumi, Y., 1986: A spectra; limited-area model with time dependent lateral boundary conditions and its application to a multi-level primitive equation model. *J. Meteor. Soc. Japan*, 64, 637-663.

Williamson, D.L., 1970: Integration of the primitive barotropic model over a spherical geodesic grid. *Mon. Wea. Rev.*, 98, 512-520.